

# *Drosophila* LAR Regulates R1-R6 and R7 Target Specificity in the Visual System

Thomas R. Clandinin,<sup>2</sup> Chi-Hon Lee,<sup>2</sup> Tory Herman, Roger C. Lee, Annie Y. Yang, Shake Ovasapyan, and S. Lawrence Zipursky<sup>1</sup>

Department of Biological Chemistry  
Howard Hughes Medical Institute  
University of California, Los Angeles  
School of Medicine  
5-748 MRL  
675 Charles Young Drive South  
Los Angeles, California 90095

## Summary

Different classes of photoreceptor neurons (R cells) in the *Drosophila* compound eye connect to specific targets in the optic lobe. Using a behavioral screen, we identified LAR, a receptor tyrosine phosphatase, as being required for R cell target specificity. In LAR mutant mosaic eyes, R1-R6 cells target to the lamina correctly, but fail to choose the correct pattern of target neurons. Although mutant R7 axons initially project to the correct layer of the medulla, they retract into inappropriate layers. Using single cell mosaics, we demonstrate that LAR controls targeting of R1-R6 and R7 in a cell-autonomous fashion. The phenotypes of LAR mutant R cells are strikingly similar to those seen in *N-cadherin* mutants.

## Introduction

Neurons elaborate complex yet precise patterns of synaptic connections during development. Growth cones navigate along highly stereotyped pathways to their targets defined by the combinatorial and sequential use of both long-range and short-range guidance signals (Tessier-Lavigne and Goodman, 1996). Upon reaching the target region, growth cones select specific cells with which to form synaptic connections. The mechanisms by which growth cones choose amongst alternative synaptic partners once they have reached the target region are poorly understood.

The stereotyped structure, detailed cellular description, and the ease of genetic manipulation of the *Drosophila* visual system make it favorable for exploring mechanisms of connection specificity. The compound eye contains some 800 simple eyes, ommatidia, each containing eight photoreceptor neurons (R cells). These cells can be divided into three classes based on their spectral sensitivity and synaptic connectivity. R1-R6 cells respond to green light and connect to targets in the first optic ganglion, the lamina. R7 and R8 cells respond to UV and blue light, respectively, and form synaptic connections in two distinct layers in the second optic ganglion, the medulla.

The precise patterns of connections in the lamina and

medulla are necessary to drive different light-dependent behaviors and form the basis of genetic screens to identify determinants of connection specificity (Lee et al., 2001). The pattern of R1-R6 connections in the lamina is complex (Braitenberg, 1967). As a consequence of the curvature of the eye and the arrangement of R cells within an ommatidium, multiple R cells distributed over the surface of the retina look at the same point in space (Kirshfeld, 1967). These groups each consist of six different neurons (i.e., an R1 in one ommatidium, an R2 in another, etc.) and form synaptic connections with the same postsynaptic targets in the lamina. By combining the synaptic inputs from multiple R cells looking at the same point in space, the sensitivity of the eye to visible light is enhanced (Laughlin et al., 1987). Genetic experiments have revealed that specific interactions between R1-R6 neurons play a key role in target selection (Clandinin and Zipursky, 2000). The connections made by R7 and R8 in the medulla are simpler than those made by R1-R6 in the lamina. The R7 and R8 cells in the same ommatidium “look” at the same point in space and terminate in retinotopic fashion in two different layers within the same column of synaptic targets in the medulla neuropil (Fischbach and Dittrich, 1989). R8 terminates within the M3 layer of the medulla and R7 terminates in a deeper layer, M6.

In this paper, we identify LAR using a behavioral screen based on the optomotor response and demonstrate that mutations in LAR lead to defects in R1-R6 and R7 connectivity. LAR encodes a receptor tyrosine phosphatase and has been shown to function in axon guidance in the fly embryo (Krueger et al., 1996; Desai et al., 1997). Using single cell mosaics, we demonstrate that LAR acts in a cell-autonomous fashion for R1-R6 and R7 specificity. LAR is required for R1-R6 axons to select amongst alternative postsynaptic targets within the lamina and in R7 for selecting between the R7 and R8 recipient layers in the medulla. This work provides evidence that LAR is required for synaptic target specificity. We show that the terminal phenotypes, expression pattern, and cellular requirements of LAR are remarkably similar to those of N-cadherin.

## Results

### Identification of Mutations Affecting R Cell Connectivity

To identify mutations disrupting R cell target selection, we undertook a genetic screen based on a sensitive behavioral assay for R cell function (Figures 1A and 1B). To enrich for mutations affecting the connections made by R1-R6 cells, we chose the optomotor response, a behavior specifically dependent upon R1-R6 function (Heisenberg and Buchner, 1977). To identify only those genes whose activities are required in R cells to mediate this response, we tested the behavior of somatic mosaic animals in which only R cells were made homozygous for mutations of interest (Newsome et al., 2000). We anticipated that this approach would identify a large

<sup>1</sup> Correspondence: zipursky@hhmi.ucla.edu

<sup>2</sup> These authors contributed equally to this work.

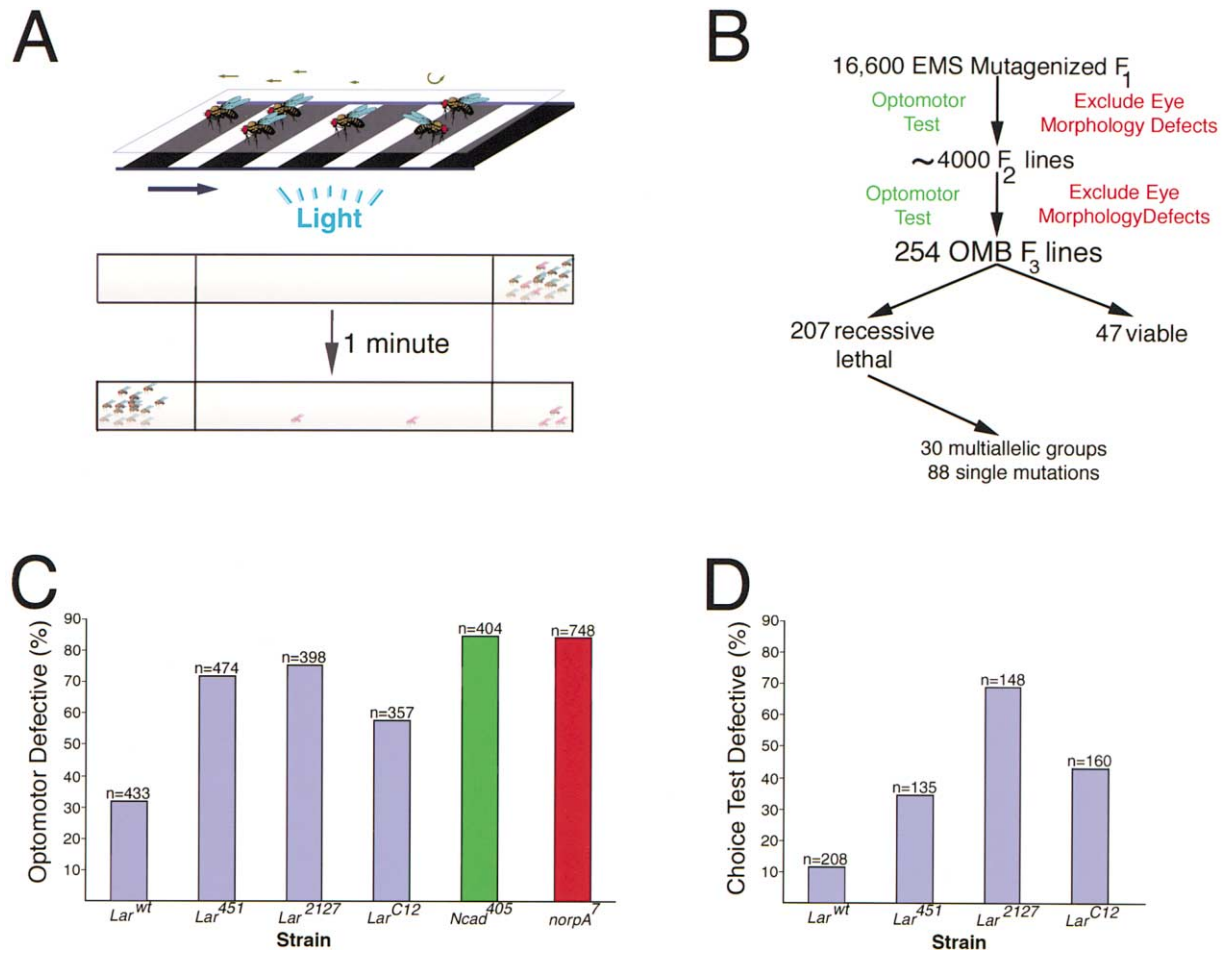


Figure 1. *LAR* Mosaic Flies Display Defects in Visual Behaviors

(A) The optomotor response apparatus. Flies shown a moving pattern of black and white stripes orient toward the apparent source of the motion and move toward it (straight arrows); mosaic flies bearing mutations that disrupt R cell function cannot detect the motion and move in random directions (curved arrows). In this test, flies are placed at one end of a long clear tube and shown the motion stimulus for 1 min; after 1 min, flies that fail to reach the terminal collection tube, a distance of approximately 27 cm (pink flies), are retained. (B) Flowchart of the optomotor response screen. Flies were mutagenized with the chemical mutagen ethylmethanesulfonate and groups of approximately 50 mosaic F<sub>1</sub> flies were tested using the optomotor response. All F<sub>1</sub> flies that failed two trials in the optomotor assay and had no defects in the external morphology of the eye were used to establish F<sub>2</sub> lines. These F<sub>2</sub> lines were then behaviorally re-tested as populations of identical flies and those groups that displayed aberrant response were retained. Of this population of 254 lines, 207 lines were homozygous lethal in nonmosaic flies, while 47 lines were homozygous viable. Pairwise combinations of the lethal mutations were tested for complementation of the lethal phenotype. (C) The optomotor response. Each genotype was divided into five groups and each group was tested twice. The y axis depicts the percentage of the population that failed to move into the terminal collection tube within 1 min (a distance of approximately 27 cm). In this assay, the response of *LAR* mosaic flies was approximately 2-fold worse than that of controls. As negative controls, a phototransduction-defective mutant, *norpA* (red bar), as well as mosaic flies bearing a strong reduction of function allele of *N-cadherin* (green bar) were tested. (D) The UV/Vis choice test. The y axis depicts the percentage of the population that chose visible light. Each genotype was divided into three or four groups and each group was tested twice. As there was little variation between trials, the results from all trials were pooled. All of the differences between the responses of *LAR* mosaic flies and control flies are highly statistically significant ( $p < 0.00001$ , Fisher's Exact Test) for both the optomotor response and the UV/Vis light choice test.

number of genes required for R cell function and, amongst this collection, we would identify a small subset required for R cell connection specificity.

Approximately 16,600 F<sub>1</sub> progeny produced by P<sub>0</sub> flies treated with the chemical mutagen EMS were tested in small groups for their optomotor response. Animals that failed to respond sufficiently to the motion stimulus within an approximately 1 min time period on two consecutive trials were recovered and used to establish lines. All F<sub>1</sub> animals and F<sub>2</sub> lines that displayed defects in the external morphology of the eye were discarded.

Individual lines were then re-tested as populations of identical flies using the optomotor response assay, and lines in which the population displayed an aberrant response were retained. From this approach, we identified 207 chromosomes that were lethal when homozygous in the entire animal and, when homozygous in the retina only, reduced or eliminated the optomotor response. We also identified 47 lines that were homozygous viable; these lines have not been further characterized.

By scoring the lethal lines for complementation of the lethal phenotype, we identified 30 loci that contain

multiple alleles, as well as an additional set of 88 loci identified by only a single mutation. These mutations affect a variety of R cell phenotypes, including differentiation, physiology, and axon extension into the optic lobe (T.R.C., C.H.L., B. Hardie, B. Zhang, C. Zuker, and S.L.Z., unpublished). The cellular bases for the behavioral effects of the remaining mutations have not been identified.

To identify mutations within this collection that affect the function of R7 (as well as R1-R6), we tested all optomotor-defective lines in somatic mosaic animals using a second visual behavioral assay specific to the function of R7, the UV/Vis light choice test (Gerresheim, 1981). From the 207 lethal lines required for R1-R6 function in mosaic animals, we identified seven mutations that cause defects in the UV/Vis light choice test in mosaic animals. Two of these are alleles of *milton* (T. Schwarz, personal communication; T.R.C., unpublished), three are alleles of an unidentified locus, one corresponds to an allele of N-cadherin (Lee et al., 2001), and one is an allele of *LAR*, *LAR*<sup>451</sup> (described below).

In this paper, we describe a detailed phenotypic analysis of *LAR*. Treisman, Dickson, and coworkers also have shown that *LAR* is required for R7 target specificity and generously provided us with two alleles, *LAR*<sup>C12</sup> and *LAR*<sup>2127</sup>, prior to publication (Maurel-Zaffran et al., 2001 [this issue of *Neuron*]). The phenotypes of these three alleles in R1-R6 and R7 connectivity and behavior are largely indistinguishable. As *LAR*<sup>451</sup> causes a severe reduction in *LAR* protein levels, it is likely that it is a strong loss-of-function allele (data not shown).

We previously reported N-cadherin's role in R cell connection specificity (Lee et al., 2001). In this paper, we include additional analysis of N-cadherin. While data for N-cadherin is shown in relevant figures, we discuss the similarities between *LAR* and N-cadherin in a separate section.

#### Loss of *LAR* Activity in R Cells Disrupts Visual Behaviors

Mosaic animals in which R cells are homozygous for reduction-of-function mutations in *LAR* display defects in both the optomotor response (R1-R6-specific; Figure 1C) and the UV/Vis light choice test (R7-specific; Figure 1D). Approximately 32% (n = 433) of mosaic flies in which R cells were homozygous for a wild-type control chromosome failed to respond to a motion stimulus, as compared to 84% (n = 748) of blind flies homozygous for a mutation in an obligatory component in the phototransduction cascade, *norpA*. Mosaic flies bearing any one of three *LAR* mutations displayed a behavioral deficit of intermediate severity, ranging from 58% (n = 357) for *LAR*<sup>C12</sup> to 72% (n = 474) for *LAR*<sup>451</sup> to 75% (n = 398) for *LAR*<sup>2127</sup>. Hence, *LAR* is required for a behavioral response dependent upon functional R1-R6 neurons.

Mosaic animals bearing these mutations in *LAR* also display defects in the R7-mediated UV/Vis light choice test. In this assay, control flies preferentially phototax toward UV light, with only 12% (n = 208) moving toward the visible light source. *LAR* eye-specific mosaic animals show defects in this response: 43% (n = 160) of *LAR*<sup>C12</sup> animals, 34% (n = 135) of *LAR*<sup>451</sup> animals, and 69% of *LAR*<sup>2127</sup> animals phototaxed toward visible light. These

results suggest that in these *LAR* mosaics, R7 function is disrupted. It is important to note that this behavioral deficit is highly sensitive to the relative light intensities used in the assay. For instance, there is little difference between control and *LAR* mutant mosaics under conditions in which the relative intensity of the UV light is increased (data not shown). In the following sections, we consider the role of *LAR* in R1-R6 and R7 target selection.

#### In *LAR* Mutants, R1-R6 Target to the Lamina

The overall R cell projection pattern in mosaic animals in which the eye, but not the target, was mutant for *LAR* was assessed using mAb24B10 staining of third instar eye-brain complexes. This antibody recognizes an R cell-specific antigen (Fujita et al., 1982). mAb24B10 staining of R1-R6 growth cones appears as a thick continuous band of staining within the lamina plexus (Figure 2A). The regular array of growth cone staining seen in the medulla is primarily associated with R8 axons as few of the later developing R7 neurons express the antigen at this stage of development. The pattern of mAb24B10 staining in *LAR* mosaic animals was largely indistinguishable from wild-type (Figure 2B). We infer that the targeting of R8 axons to the medulla is normal in *LAR* mosaic animals at this stage. Staining of *LAR* mosaics with an R4-specific marker reveals a regular pattern of R cell growth cones in the lamina plexus similar to wild-type (data not shown), indicating that initial topographic mapping to the lamina is normal. Using an R2-R5-specific marker, we assessed lamina versus medulla targeting. A small fraction of these neurons extended beyond the lamina plexus (Figures 2C and 2D) as compared to other mutants with R1-R6 targeting phenotypes (Garrity et al., 1999; Poeck et al., 2001; Rao et al., 2000; Senti et al., 2000). As in wild-type, R7 axons, as visualized using an R7-specific marker, elaborate a topographic map in the medulla neuropil (Figures 2E and 2F; see below). *LAR* was not required in R cells for glial cell development (data not shown). R cell fate determination and differentiation appeared normal as assessed using various cell type-specific markers in the developing larva and morphological criteria observed in plastic sections of the adult eye stained with toluidine blue (data not shown).

#### *LAR* Is Required for R1-R6 Axons to Choose Appropriate Targets within the Lamina

To determine whether the defects in R1-R6 function observed in *LAR* mosaic animals reflect defects in the specific pattern of connections made by R1-R6 axons within the lamina, we assessed R1-R6 cell connection specificity in mosaic flies. In wild-type animals during the third larval stage, R1-R6 axons from each ommatidium extend into the optic lobe as a single fascicle and terminate together as a tight cluster. During mid-pupal development, individual growth cones extend outward from the bundle and across the surface of the lamina plexus, to make synaptic connections with axons from a single column of lamina target neurons (Meinertzhagen and Hanson, 1993). The result of this process is that R cell axons from a single ommatidium choose targets arranged in an invariant pattern (Figure 3A).

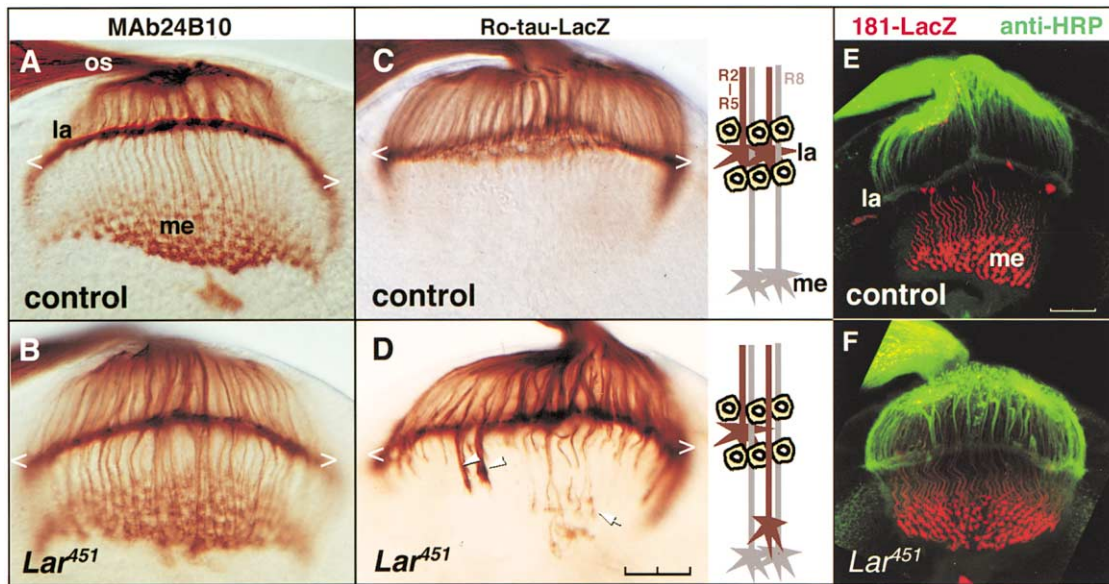


Figure 2. The Initial R Cell Projections in *LAR* Mutants Are Largely Normal

(A, C, and E) Wild-type. (B, D, and F) *LAR*<sup>451</sup> eye-specific mosaic animals. The developing optic lobe was assessed at the late third instar (A–D) and the prepupal stage (E and F). Chevrons denote the position of the laminal plexus. os, optic stalk; la, lamina; me, medulla. (A and B) R cell projections were visualized using mAb24B10. (A) R1–R6 axons project into the optic lobe and terminate in the lamina plexus (seen as a smooth, uniform line between the chevrons), while the R8 axons project through the lamina and form a regular array of expanded growth cones in the medulla. In *LAR*<sup>451</sup> mosaic animals (B), the overall R cell projections are largely indistinguishable from wild-type. (C and D) Targeting of R1–R6 to the lamina was assessed using an R2–R5-specific marker, Ro-tau-lacZ. In wild-type, all R2–R5 axons target to the lamina (C). However, in *LAR* mosaic animals (D), a small number of R2–R5 axons overshoot the lamina and terminate aberrantly in the medulla (arrow). Some of these axons form larger fascicles (arrowhead). Insets: schematic summaries of (C) and (D). (E and F) Optic lobes were stained using an R7-specific marker, PM181-lacZ (red), and a neuron-specific marker anti-HRP (green). In both wild-type (E) and *LAR*<sup>451</sup> mosaic animals (F), the expanded R7 growth cones form a regular array of 8–10 rows in the medulla. Scale bars: 20  $\mu$ m in (D) and (E).

The pattern of targets selected by R1–R6 neurons can be visualized by injecting Dil into single ommatidia to fluorescently label R cell membranes (Clandinin and Zipursky, 2000; Figures 3B–3D). In *LAR* mosaics, mutant axons almost always fail to extend outward from the ommatidial bundle toward their normal synaptic partner (Figure 3C). In *LAR*<sup>C12</sup>, *LAR*<sup>2127</sup>, and *LAR*<sup>451</sup> mosaic flies, 0/54, 1/78, and 10/60 R cell axons extended, respectively. R cell growth cones that failed to leave the bundle were abnormally thin and displayed few filopodia. We also observed rare cases in which R1–R6 axons from *LAR* mutant ommatidia failed to stop within the lamina, and terminated instead within a deeper brain layer consistent with the results observed in third instar using the R2–R5 marker (data not shown).

We assessed R cell topographic mapping at 40% pupal development using mAb24B10. In wild-type, R cell axons that have selected their target neurons form a regular “checker-board” pattern of terminals (Figures 3E and 3F). In *LAR* mosaics, this pattern is mildly disrupted (Figures 3E and 3G). Therefore, the R cell targeting defects in the lamina plexus seen in *LAR* mutant mosaics are unlikely to be an indirect result of errors in topographic mapping.

#### **LAR Is Required Cell Autonomously for R1–R6 Cell Connection Specificity**

To address whether *LAR* is required within individual R1–R6 cells to select targets, we developed a mosaic

method to study the projections of individual mutant R cells in the adult (Figure 4A). In these experiments, the vast majority of R cell axons, as well as all target neurons, are heterozygous (and presumably phenotypically wild-type). This method is based upon the MARCM system (Lee and Luo, 2001) that has been further modified for use in R cell axons (Lee et al., 2001); in this work, we modify it further to study R1 and R6 axons specifically. Briefly, we use a GMR promoter fused to a recombinase, FLP, which directs expression of the recombinase posterior to the morphogenetic furrow and results in approximately 10%–15% of R1, R6, and R7 cells becoming homozygous for a particular chromosome (see Experimental Procedures). To label these cells, we place a ubiquitously expressed Gal80 construct in *trans* to the homologous chromosome bearing either a control chromosome or a mutation in *LAR*. Cells that undergo mitotic recombination and become homozygous for *LAR* lose the Gal80 construct and can then be labeled using a cell type-specific Gal4 promoter. In this case, we use the Rh1 opsin promoter fused to Gal4 to drive expression of a cytoplasmic lacZ reporter to label cells that have undergone mitotic recombination; all other R cell axons are stained with mAb24B10.

In wild-type animals bearing a control chromosome, cross-sectional views of the lamina immediately distal to the lamina plexus reveal an array of R cell axon bundles corresponding to R cell axons from individual ommatidia. At this level, axons from R cells that have under-

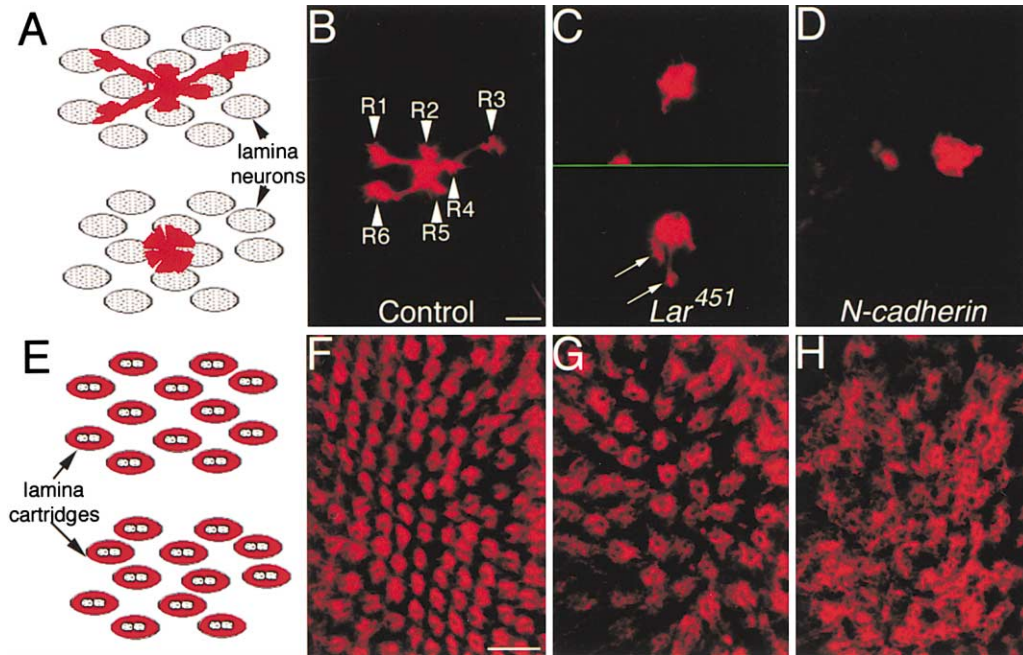


Figure 3. LAR Is Required for R1-R6 Axons to Choose the Appropriate Pattern of Targets in the Lamina

(A) Schematic display of the R1-R6 connection pattern in the lamina. R1-R6 axons (red) from a single ommatidial bundle extend through the lamina and stop at lamina target neurons (black stippled ellipses) arranged in an invariant pattern (upper schematic). In mosaic animals bearing mutations in either *LAR* or *N-cadherin*, R cell growth cones fail to extend out of the ommatidial bundle (lower schematic). (B–D) Dil-labeled projections of R cell axons from single ommatidia. (B) R cell axons in control animals extend outward in an invariant pattern and can be identified by their characteristic morphology. (C) R cell axons in *LAR* mutant mosaics fail to extend out of the ommatidial bundle. Shown in the upper panel is an example in which no R cell axons extended; in the lower panel is an example in which two extensions were observed (arrows). (D) R1–R6 axons in *N-cadherin* mosaics display lamina targeting phenotypes similar to those seen in *LAR* mosaics. (E) Schematic display of the arrangement of R cell termini within the lamina plexus during mid-pupal development. R cell axons (red) form a regular array of bundles in wild-type animals (upper schematic); the holes within each bundle correspond to the positions of axons extending from lamina target neurons. In *LAR* mutants, this array is only slightly disrupted (lower schematic). The apparent discrepancy in the density of cartridges between wild-type and *LAR* is, at least partially, due to differences in section plane. (F–H) Cross-sectional views of the lamina plexus stained with an R cell-specific marker mAb24B10 (red). (F) Wild-type. (G) *LAR* mosaic eye. (H) *N-cadherin* mosaic eye. In *N-cadherin* mosaic eyes, the topographic map of the lamina plexus is severely disrupted (see Lee et al., 2001). Scale bars: 5  $\mu\text{m}$  in (B)–(D); 10  $\mu\text{m}$  in (F)–(H).

gone mitotic recombination are visible as small dots of lacZ staining associated with a single bundle that correspond to a single R cell axon within the fascicle. At a slightly more proximal level, these lacZ-positive fibers invariably extend across the surface of the lamina where they then turn approximately 90° and thicken, forming the presynaptic structure ( $n = 20$ ; Figures 4B–4F). In single fibers mutant for *LAR*, we observe that some 50% (11/23) fail to extend out from the ommatidial bundle before elaborating the presynaptic terminal (Figure 4B, purple arrows and arrowheads in [G] and [H]). That is, in these cases, the *LAR* mutant axon elaborated a presynaptic terminal in an inappropriate position. In 12/23 cases, the fiber did extend to an apparently normal position before thickening (Figure 4B, white arrows and arrowheads in [G], [I], and [J]). These results demonstrate that *LAR* activity is required cell autonomously within R1 and R6 (and likely within R2, 3, 4, and 5) for these axons to choose synaptic targets in the appropriate position.

At the resolution of the marker scheme used in this analysis, the morphology of the presynaptic termini in *LAR* mutant R cell axons is largely normal. In wild-type animals, individual R1–R6 axons form a thick terminus that extends throughout the lamina plexus and remains

associated with a single target cartridge (Figures 4O and 4P). In *LAR* mutant axons, these termini extend into the lamina plexus but are somewhat more irregular in thickness than the corresponding controls (Figures 4Q, 4R, and data not shown). Hence, this gene may also play some role in synapse formation, but it remains possible that these minor defects in terminal arbor morphology are an indirect result of an earlier defect in synaptic partner choice.

#### ***LAR* Is Required Cell Autonomously to Regulate R7 Targeting**

The observation that *LAR* affects the UV/Vis choice test supports the notion that in *LAR* mutants, R7 connectivity is disrupted. To determine whether *LAR* functions cell autonomously in R7 to control target layer specificity, we generated single *LAR* mutant R7 axons that are surrounded largely by wild-type R cell axons and a wild-type target (Figures 5A, 5B, and 5E–5H). Mutant R7 axons were visualized using a synaptic marker, synaptobrevin-GFP (see Lee et al., 2001). Unlike wild-type R7 axons which terminate precisely at the M6 layer (Figures 5A and 5B), the single *LAR* mutant R7 axons frequently mistarget to the M3 layer or terminate at variable positions in the medulla neuropil between M3 and M6 (Fig-

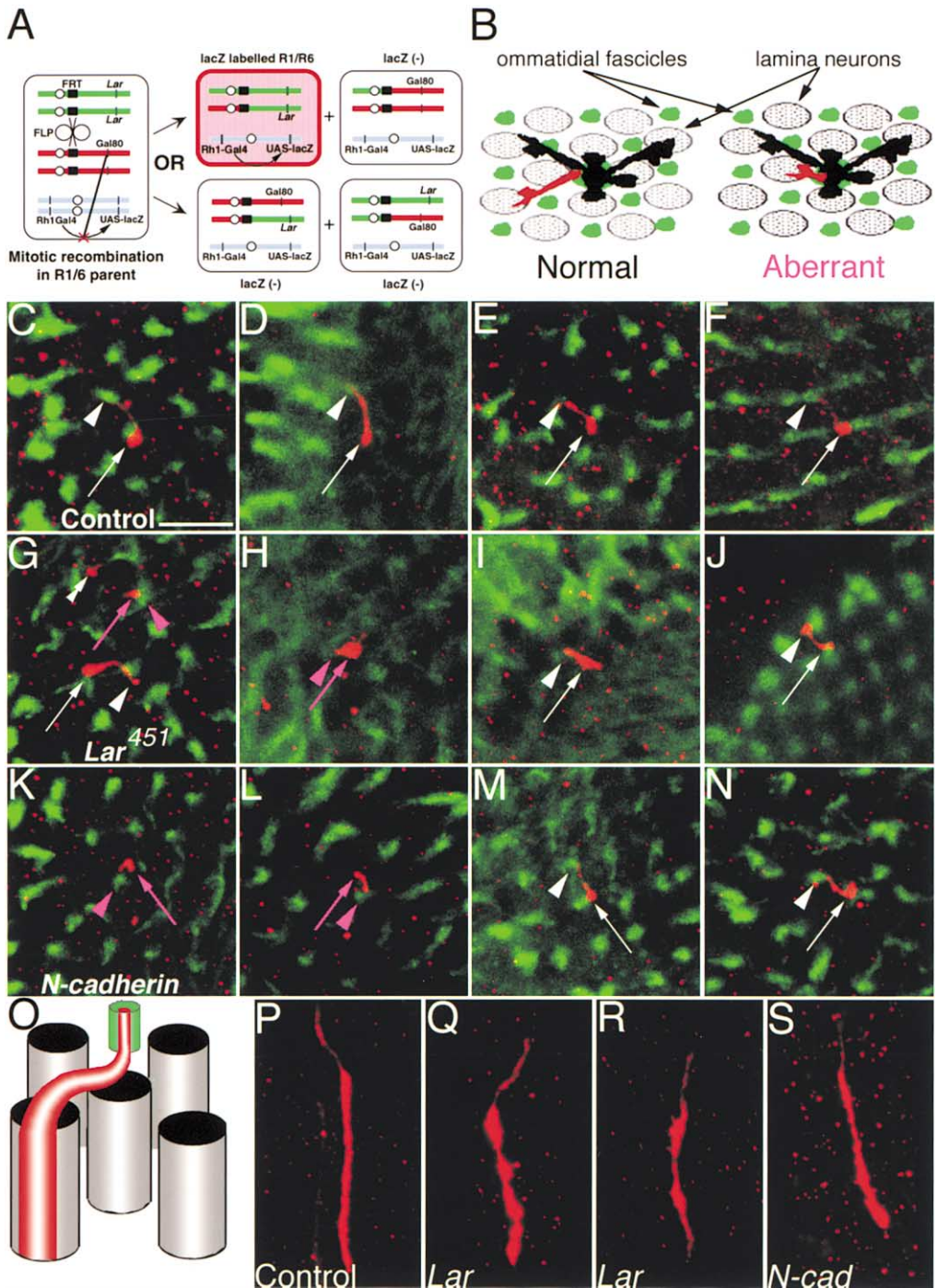


Figure 4. Single Mutant *LAR* and *N-Cadherin* R1 and R6 Axons Target Inappropriately within the Lamina

(A) Schematic outline of the MARCM method for generating single mutant R1 and R6 cells in the adult (see text). These axons were visualized using an antibody to lacZ (red), driven under the control of the R1-R6-specific Rh1 promoter. (B) Schematic of the R1-R6 connection pattern in the lamina, viewed from the top. Individual R1 and R6 axons (labeled with lacZ, red) homozygous for a control chromosome extend out from the ommatidial bundle (labeled with the R cell-specific antibody mAb24B10, green) toward their lamina targets (unstained, stippled gray). All other R cell axons from the same ommatidium are not visualized (black). Individual mutant R1 and R6 axons fail to extend away from the ommatidial bundle (left panel). (C–N) Top views of individual labeled R cell axons within the lamina plexus. Each axon originates at a single ommatidial bundle (arrowhead) and extends across the surface before elaborating a presynaptic thickening (arrow). Axons that extended normally are indicated by white arrows; those that failed to extend are marked in purple. (C–F) Wild-type. (G–J) *LAR*. (K–N) *N-cadherin*. (O) Schematic illustration of a single marked R cell axon viewed from the side. Each R cell axon (red) elaborates a presynaptic structure within a single cartridge within the lamina plexus (gray columns). The ommatidial bundle is indicated in green (unstained in [P]–[S]). (P–S) Side views of single R cell axons within the lamina plexus. (P) Wild-type. (Q and R) *LAR*. (S) *N-cadherin*. The morphology of presynaptic terminals of *LAR* and *N-cadherin* mutant axons is somewhat irregular (see text). Scale bar: 10  $\mu$ M.

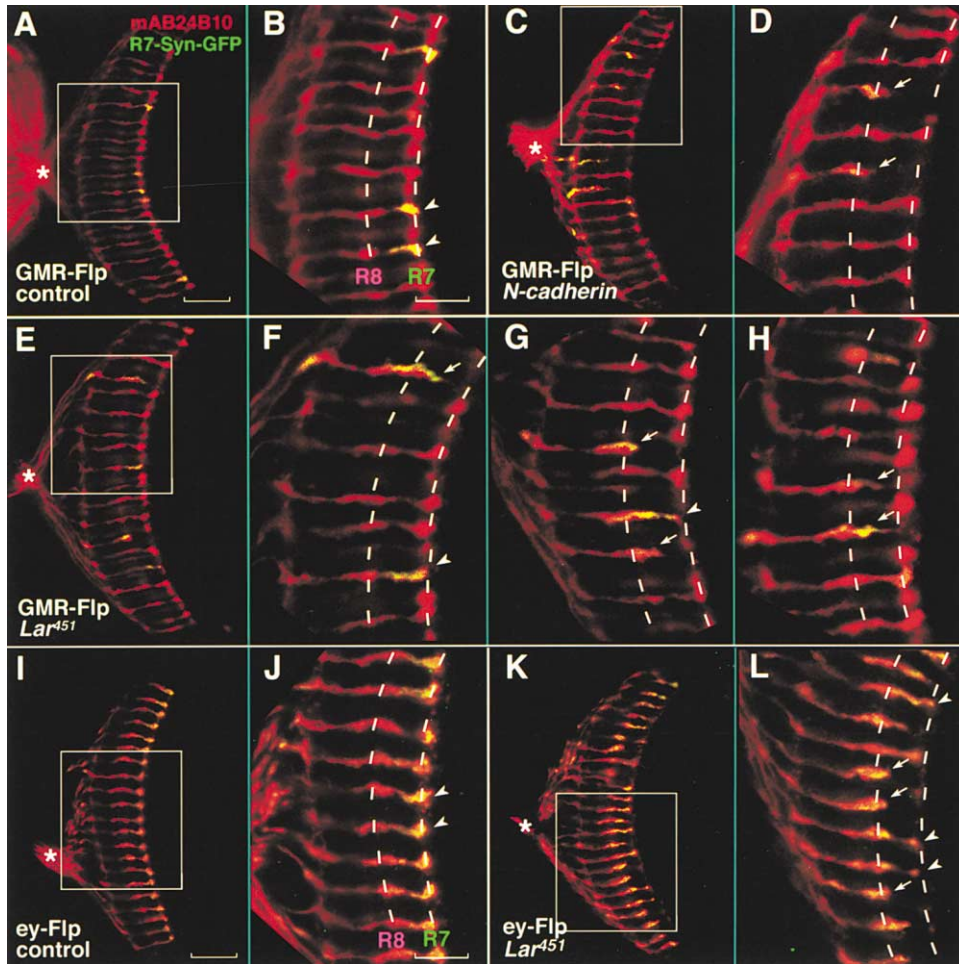


Figure 5. LAR Is Required Cell Autonomously in R7 for Target Selection

R7 targeting was assessed in adult flies. (A–H) Single mutant R7 cells were generated using GMR-FLP-mediated mitotic recombination (see text and Lee et al., 2001). These R7 axons were labeled using the MARCM system and synaptobrevin-GFP (green). The R7 and R8 axons were visualized using mAb24B10 (red). (I–L) Eye-specific mosaic animals in which the retina alone is homozygous for *LAR*<sup>451</sup>. R7 and R8 axons were visualized using synaptobrevin-GFP (green) and mAb24B10, respectively. (A, B, I, and J) Wild-type. (C and D) *N-cadherin*. (E–H, K, and L) *LAR*<sup>451</sup>. (A, C, E, I, and K) Low magnification view of medulla. Boxes indicate region displayed in (B), (D), (F), (J), and (L) at higher magnification. \*, optic chiasm. In (B), (D), (F)–(H), (J), and (L), dash lines denote the R7 and R8 recipient layers. (A and B) Single R7 cells, homozygous for a wild-type FRT40 chromosome arm, terminate at the R7 recipient layer. (C and D) Single *N-cadherin* mutant R7 axons mistarget to the R8 recipient layer. (E–H) Single *LAR*<sup>451</sup> mutant R7s fail to terminate at the R7 recipient layer and stop instead at the R8 recipient layer or in the region between these two layers (arrows). Some *LAR* mutant R7s reach the R7 recipient layer, but their termini assume abnormal morphology (arrowhead). (I–L) In *LAR* eye-specific mosaic animals, similar R7 mistargeting defects were observed. In both control (I and J) and *LAR*<sup>451</sup> mutant mosaic animals (K and L), the overall topographic map is normal. Scale bars: 20  $\mu\text{m}$  in (A), (C), (E), (I), and (K); 10  $\mu\text{m}$  in (B), (D), (F)–(H), (J), and (L).

ures 5E–5H). In particular, 68% ( $n = 125$ ) and 74% ( $n = 85$ ) of *LAR*<sup>451</sup> and *LAR*<sup>2127</sup> mutant R7s, respectively, fail to target to M6. Although the remaining mutant R7 axons terminate at the appropriate layer, the morphology of the termini is clearly abnormal. In contrast to the wild-type button-like appearance, mutant R7 termini assume an abnormal spear-like morphology. The expressivity of the mistargeting phenotype seen in single cell and whole eye mosaics (Figures 5I–5L) is quantitatively similar, as in *LAR*<sup>451</sup> and *LAR*<sup>2127</sup> eye-specific mosaics we observed 78% ( $n = 291$ ) and 81% ( $n = 389$ ) mistargeted R7 axons, respectively. We observed similar expressivity of the R7 mistargeting phenotype in *LAR* eye-specific mosaics using synaptobrevin-GFP, mAb24B10, or  $\beta$ -galactosi-

dase under the control of the glass promoter as markers of the R7 axon. Hence, it is unlikely that the targeting defects described with synaptobrevin-GFP reflect defects in intracellular targeting of the marker.

#### LAR and N-Cadherin Appear to Control Similar Steps in R Cell Targeting

The functional requirements for LAR in R1–R6 and R7 targeting are remarkably similar to those for N-cadherin (Lee et al., 2001). Loss of N-cadherin activity from R cells causes behavioral deficits similar to those seen in *LAR* mutant mosaics (Figures 1C and 1D). In eye-specific mosaics in which R cells are homozygous for loss-of-function mutations in *N-cadherin*, R1–R6 axons fail to

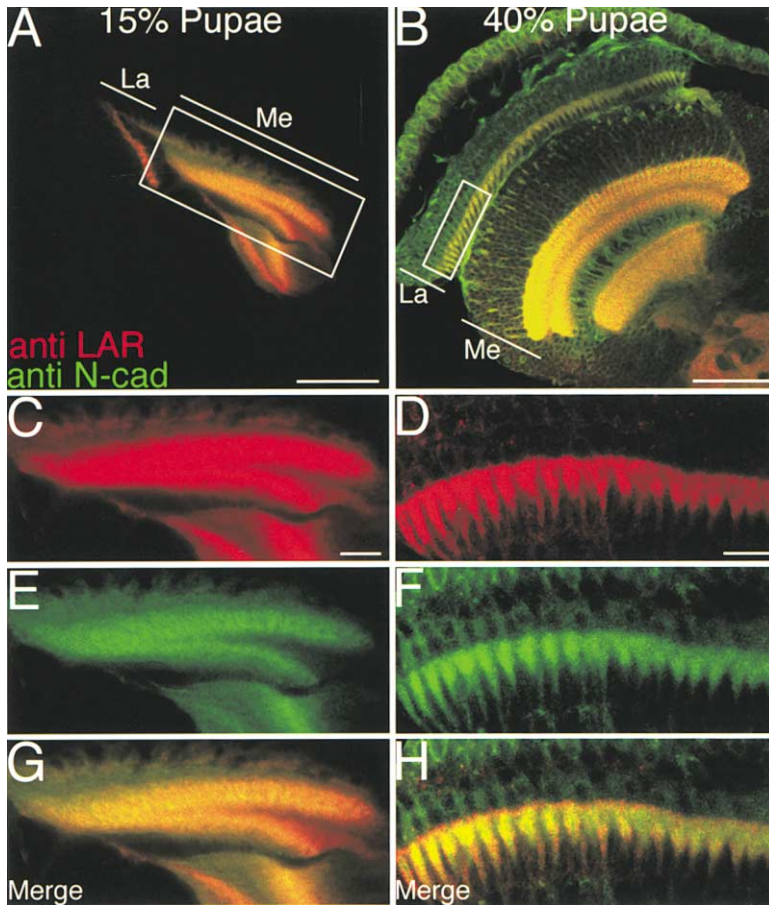


Figure 6. LAR and N-Cadherin Display Overlapping Patterns of Expression in the Optic Lobe

LAR (red) and N-cadherin (green) expression was assessed both during early pupal development (15%, when R7 axons are targeting in the medulla, panels [A], [C], [E], and [G]) and during mid-pupal development (40%, when R1-R6 axons are targeting in the lamina, panels [B], [D], [F], and [H]). Both LAR and N-cadherin are broadly expressed at both developmental stages. La: lamina. Me: medulla. (A) Low magnification view of the optic lobe at 15% pupal development. White box denotes the region of the medulla displayed in (C), (E), and (G). Scale bar: 40  $\mu$ m. (B) Low magnification view of the optic lobe at 40% pupal development. White box denotes region of the lamina displayed in (D), (F), and (H). (C and D) LAR expression. (E and F) N-cadherin expression. (G and H) Merge. Scale bars in (C)–(H): 10  $\mu$ m.

extend out of the ommatidial bundle (Figure 3D). We previously demonstrated that *N-cadherin* acts in a cell-autonomous fashion to control R7 targeting. *N-cadherin* mutant R7 axons frequently terminate in the R8 recipient layer (M3) rather than in their normal target layer (M6). This mistargeting phenotype occurs with comparable frequency to the targeting errors observed in LAR mutant R7 axons (Figures 5C and 5D). In addition, there are subtle differences in the targeting of LAR and *N-cadherin* mutant R7s; in LAR, but not in *N-cadherin*, R7 axons frequently terminate between M3 and M6 (see below).

To further compare the R1-R6 phenotype of N-cadherin and LAR, individual R cell axons were made homozygous for a mutation in *N-cadherin*. R1 and R6 cells mistargeted in a manner to that observed for single LAR mutant axons. In particular, 14/28 *N-cadherin* mutant axons failed to extend away from the ommatidial fascicle before elaborating a presynaptic structure (Figures 4K and 4L), while the remainder (14/28) extended normally (Figures 4M and 4N). As in LAR, the morphology of the presynaptic terminus in single *N-cadherin* mutant R1 and R6 cells is only mildly disrupted (Figure 4S). N-cadherin does play additional roles in R cell targeting that are not dependent on LAR activity. For example, N-cadherin, but not LAR, is required for the formation of the normal topographic map of R cell axons in the lamina and medulla (Lee et al., 2001; Figure 3H).

The patterns of LAR and N-cadherin expression seen in the optic lobe during pupal development are largely overlapping (Figure 6). LAR and N-cadherin are broadly

expressed in the optic lobes during late larval and pupal development (Figure 6 and data not shown). Strong LAR and N-cadherin protein expression on R1-R6 axon termini was observed within the lamina plexus (Figures 6A, 6B, 6D, 6F, and 6H). We also observed expression in the layers of the medulla that contain the R7 and R8 termini, as well within other regions of the optic lobe (Figures 6A, 6B, 6C, 6E, and 6G).

#### LAR Mutant R7 Growth Cones Project to the Appropriate Layer but Then Retract to the R8 Layer

Since LAR eye mosaics show striking R7 targeting defects at the adult stage (Figures 5I–5L), we examined R7 targeting at two different stages of pupal development (Figure 7). To visualize R7 growth cones at early stages of development we used an early R7-specific promoter (PM181) driving the expression of  $\beta$ -galactosidase (Lee et al., 2001). In early pupa, R7 and R8 termini form a developmental gradient across the medial/lateral axis of the medulla (from left to right in Figure 7). Each R8 axon, visualized with mAb24B10 staining, arrives at the lateral edge of the medulla neuropil where it terminates in a superficial layer. Some 14 hr later (corresponding to 7–9 rows of R cell projections), the R7 axon from the same ommatidium reaches the medulla and extends beyond the R8 terminus to the presumptive R7 recipient layer (Figures 7A and 7B). Within 5–8 hr (corresponding to 3–4 rows), the distance between the R7 and R8 growth

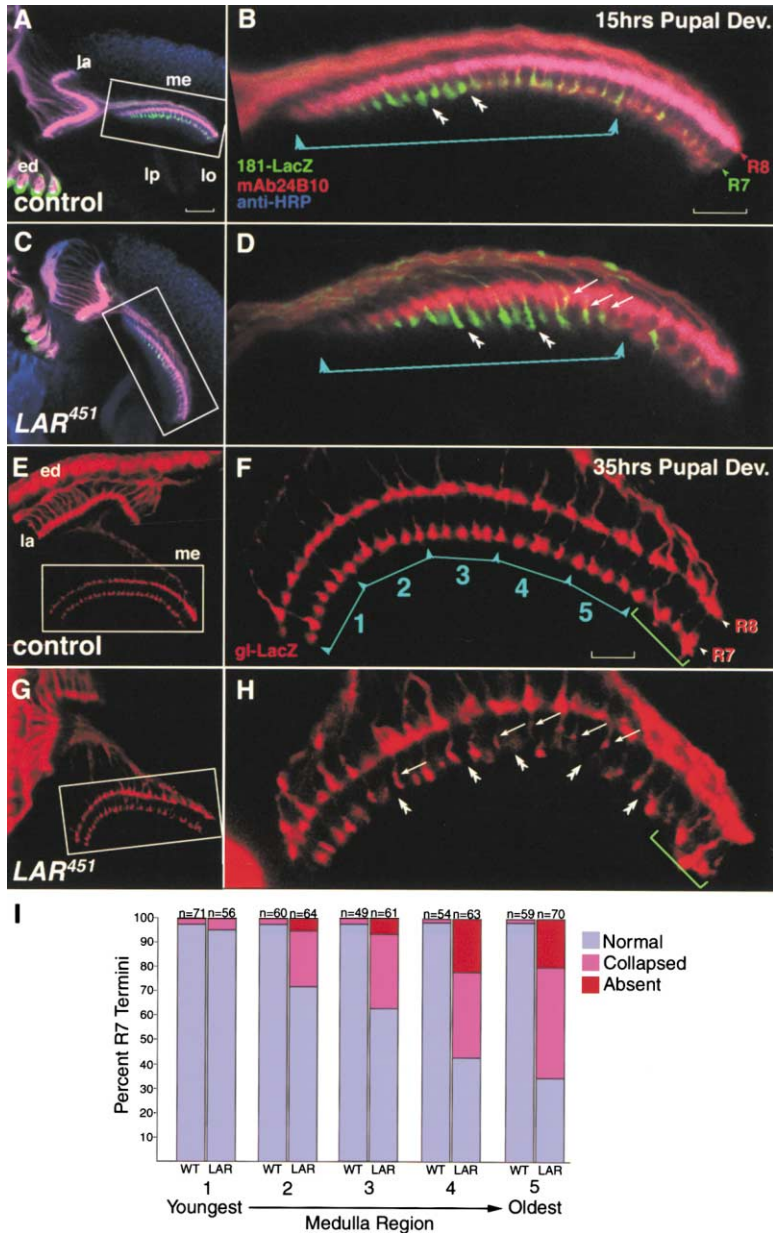


**Figure 7. *LAR* Mutant R7 Axons Initially Target to the R7 Recipient Layer but Later Retract to the R8 Recipient Layer**

R7 targeting was assessed in the developing optic lobes of eye-mosaic animals at 15 hr after pupation (A–D) and at 35 hr after pupation (E–I). In (A)–(D), R7 axons were labeled using PM181-Gal4, UAS-lacZ, and visualized with anti-lacZ antibody (green). The R8 and mature R7 axons (but not younger R7 axons) were stained with mAb24B10 (red). Anti-HRP antibody stains the axons and the developing neuropils to give an outline of the developing optic lobe (blue). In (E)–(H), all R cell axons were labeled using lacZ under the control of the *glass* promoter and visualized with an anti-lacZ antibody. The R7 and R8 recipient layers are indicated. ed, eye disk; la, lamina; me, outer medulla; lp, lobula plate; lo, lobula. (A and C) Cross-section of developing optic lobe. The boxed regions, comprising the medulla, are shown at higher magnification in (B) and (D), respectively. (B and D) In this view of the medulla, the newly arriving R7 growth cones are to the left and more mature R7 growth cones are to the right. Since the expression of lacZ driven by the PM181-Gal4 driver diminishes in older R7 axons, we consider only the most recently arrived R7 axons (underlined regions in [B] and [D]). (A and B) In wild-type, the R7 growth cones immediately extend beyond the R8 layer and exhibit a button-like expanded morphology (double arrowhead) 5–8 hr after innervating the medulla. In *LAR*<sup>451</sup> mutant animals (C and D), R7 growth cones also extend beyond the R8 layer and assume an abnormal bush-like structure (double arrowhead). In the older part of the medulla, some R7 growth cones fail to stay in the R7 recipient layer and retract toward the R8 recipient layer (arrows). (E and G) Low magnification cross-sections of the optic lobe at 35 hr after pupation. The boxed regions are displayed at high magnification in panels (F) and (H), respectively. In this orientation, the youngest, most anterior region of the medulla is to the left. In wild-type animals, R7 terminals form a regularly spaced array in the R7 layer and display a characteristic morphology. In *LAR* eye mosaics, the R7 layer contains gaps (double arrowheads) reflecting loss of R7 terminals as well as R7 terminals

that display an aberrant, collapsed morphology (arrows). To quantify this phenotype, we divided the medulla into five equally sized regions, in which region 1 contains the youngest R7 axons, and region 5 contains the oldest. Using serial optical sections, we then counted and classified R7 terminals in the presumptive R7 recipient layer in each region as either normal, collapsed, or absent (panel I). We excluded the most posterior, oldest region of the medulla (white line) from this analysis because these oldest R cells are unlikely to be mutant for *LAR* (C-H.L. and S.L.Z., unpublished). At this stage of development, the severity of the *LAR* phenotype correlates with the age of the R7 axons: older R7 axons tend to be more frequently disrupted. These results suggest that while *LAR* mutant R7 axons do target to the R7 layer, they are unable to maintain stable contact and withdraw from the layer throughout pupal development. Scale bars: 20  $\mu$ m in (A), (C), (E), and (G); 10  $\mu$ m in (B), (D), (F), and (H).

cone termini increases as the intervening region of the medulla expands by intercalary growth of processes from lamina and medulla neurons. In *LAR* eye mosaics, R7 growth cones extend beyond the R8 layer (Figures 7C–7F). These growth cones exhibit abnormal morphology, with elongated bush-like structures. Toward the older part of the developing medulla, R7 growth cones terminate at various levels between, and including, the R7 and R8 recipient layers. As we do not observe R7 growth cones terminating in the R8 layer in younger

regions of the medulla, we infer that some R7 growth cones retract processes to the R8 recipient layer. Since young R7 growth cones exhibit aberrant morphology, we cannot rule out the possibility that the retraction defect reflects an earlier defect in R7 recognition of determinants in the R7 recipient layer.

This retraction phenomenon continues into later stages of pupal development. We used confocal microscopy in whole-mount preparations of mid-pupal brains in which R cell axons were labeled with  $\beta$ -galactosidase

under the control of the glass promoter. In wild-type animals, we observed that R7 termini lie in precise rows and almost invariably displayed a distinctive expanded morphology. By contrast, in *LAR* eye mosaics, we observed that individual rows of termini contain gaps, reflecting R7 axons that have mistargeted. In addition, those R7 termini that were present in the R7 layer frequently displayed an aberrant, "collapsed" morphology, in which only a thin process remained at the normal termination site. We hypothesize that these collapsed termini are in the process of retracting from the R7 layer. Consistent with the idea that these defects in R7 morphology reflect an ongoing retraction process, we found that the expressivity of these defects correlated strongly with the age of the R7 terminus. That is, in younger regions of the medulla, few aberrant R7 terminals were observed, while in older regions of the medulla, the majority of R7 axons were affected. Moreover, in the oldest regions of the medulla, the fraction of R7 terminals that had either retracted from the R7 layer or displayed a collapsed morphology was approximately equal to the fraction of mistargeted R7 axons we observed in adult animals. Taken together, these experiments demonstrate that *LAR* mutant R7 axons initially extend past the R8 layer into the presumptive R7 layer and then retract as development proceeds. For technical reasons, we are unable to extend these developmental analyses to single mutant R7 axons in an otherwise wild-type background.

## Discussion

Different classes of R cell axons elaborate distinct patterns of synaptic connections in the optic ganglia (Meinertzhagen and Hanson, 1993). Here we demonstrate at the level of single identified cells that the receptor tyrosine phosphatase *LAR* is required for the selection of synaptic targets by two classes of R cell axons, R1-R6 and R7. *LAR* mutant R1-R6 growth cones select inappropriate targets in the lamina. Similarly, *LAR* mutant R7 axons frequently terminate in the wrong synaptic layer within the medulla. Although *LAR* mutant R7 axons initially project beyond R8 termini, as in wild-type, they frequently retract to the R8 recipient layer.

### **LAR Regulates R1-R6 and R7 Target Specificity**

*LAR* is required cell autonomously within R1-R6 cells for their growth cones to extend out of the ommatidial bundle and toward their postsynaptic targets. Genetic studies have demonstrated that interactions amongst R cells are required for R cell target selection. Serial electronmicrographic reconstruction studies revealed that R1-R6 growth cones undergo stereotyped morphological changes, including a specific sequence of contacts between them, prior to extension from the fascicle (Meinertzhagen and Hanson, 1993). During this process, each R1-R6 growth cone acquires a unique polarity directed toward its target. This polarity may be a major determinant of target selection. *LAR* may be required for interactions between R cell axons to establish polarity or for extension from the bundle to specific targets. Intriguingly, recent results have suggested that *LAR* may play a direct role in controlling the polarity of the actin

cytoskeleton in follicle cells in the *Drosophila* ovary (Bateman et al., 2001). Alternatively, *LAR* may mediate interactions between R cell growth cones and lamina neuronal targets. Whatever the mechanism, it should be emphasized that these are highly local interactions with each R cell projecting between 2 and 10  $\mu\text{m}$  from the bundle to its target.

*LAR* is also required for R7 neurons to select the appropriate target layer within the medulla neuropil. Most *LAR* mutant R7 neurons terminated at positions distal to their normal target layer in mosaic adults in which the entire eye or a subclass of R7s were rendered homozygous for *LAR*. Developmental analysis revealed that *LAR* mutant R7 growth cones initially extend past R8 largely as in wild-type and exhibit aberrant morphologies. *LAR* mutant growth cones show an elongated structure frequently spanning the 3–5  $\mu\text{m}$  separating the R7 and R8 recipient layers. In older regions of medulla, many *LAR* mutant R7 growth cones retract to the R8 layer. These developmental defects correlate with the phenotypes observed in the adult. While it is possible that *LAR* mediates interaction between the R7 and R8 growth cones, we favor a model in which *LAR* is required on the R7 growth cone to mediate interactions with the R7 recipient layer.

### **PTP69D and LAR Have Distinct Functions in R Cell Targeting**

Previous work demonstrated that another receptor protein tyrosine phosphatase, PTP69D, is required for R cell targeting. In PTP69D eye-specific mosaics, some 25% of the R1-R6 axons fail to terminate in the lamina (Garrity et al., 1999). In addition, approximately 47% of R7 axons mistarget to the R8 layer in the medulla (Newsome et al., 2000). In *LAR* mutant mosaics, less than 5% of R1-R6 axons fail to terminate in the lamina while the majority (approximately 70%) of R7 axons mistarget to the R8 layer. These results suggest that PTP69D and *LAR* have both distinct and overlapping roles in R cell targeting. These data are consistent with previous studies of RPTP function in the fly embryo. While RPTPs have been shown to regulate fasciculation, axon extension, and midline crossing in the embryo (Krueger et al., 1996; Desai et al., 1996; and reviewed in Van Vactor, 1998), our studies in visual system demonstrate that *LAR* also is required for target selection. Based on loss-of-function phenotypes and genetic interactions, RPTPs have been proposed to modulate the activity of the Robo receptor at the midline (Sun et al., 2000). In support of a modulatory role for *LAR* in regulating receptor function, genetic and biochemical studies in vertebrates have demonstrated that *LAR* negatively regulates insulin receptor function (Ren et al., 1998; Zabolotny et al., 2001; Tsujikawa et al., 2001). Alternatively, RPTPs may recognize distinct extracellular guidance or targeting signals. Indeed, the laminin-nidogen complex has been shown to bind to vertebrate *LAR* (O'Grady et al., 1998).

### **LAR May Directly Regulate N-Cadherin Activity**

Based on the similarities between the N-cadherin and *LAR* targeting phenotypes, their cellular requirements, and their distributions, we propose that they act to-

gether to control R cell targeting. While our genetic analysis does not provide insights into whether LAR and N-cadherin function in the same molecular pathway, biochemical studies in vertebrate cell culture support an intimate relationship between them. Vertebrate LAR, as well as LAR family RPTPs (RPTP $\mu$ , RPTP $\kappa$ , and RPTP $\delta$ ) physically associate with an N-cadherin-catenin complex and regulate the phosphorylation of  $\beta$ -catenin (Kypta et al., 1996; Brady-Kalnay et al., 1998). Phosphorylation of  $\beta$ -catenin is thought to inhibit its function downstream from cadherins. Hence, LAR family RPTPs may act as positive regulators of N-cadherin function. That these interactions are of functional significance is suggested by studies on chick retinal ganglion cell axons in vitro in which RPTP $\mu$  promotes N-cadherin-mediated outgrowth (Burden-Gulley and Brady-Kalnay, 1999). Furthermore, genetic interactions between *Abl*, encoding a cytoplasmic tyrosine kinase and *armadillo* (the fly  $\beta$ -catenin) (Loureiro and Peifer, 1998), as well as both biochemical and genetic interactions between LAR and *Abl* (Wills et al., 1999), provide additional support for interaction between N-cadherin and LAR in axon guidance in the developing fly embryo. These observations lead to the intriguing view that LAR-mediated signaling events modulate the N-cadherin-dependent homophilic binding activity between R cell afferents, or between them and their targets, thereby playing a key role in regulating connection specificity. Alternatively, N-cadherin and LAR could function in parallel with N-cadherin acting through  $\beta$ -catenin and LAR acting through its direct association with other signaling components such as *Abl* and the cytoskeletal regulator, *Ena*.

#### Experimental Procedures

##### Genetics

Fly stocks were maintained on standard medium at 22°C unless stated otherwise. Chemical mutagenesis was performed using ethylmethane sulfonate under standard conditions (Ashburner, 1989; Grigliatti, 1986). For our screen, eye-specific mosaic flies were generated using the FLP/FRT system in which FLP is under the control of an eyeless promoter fragment, and a recessive cell lethal mutation (*cyc<sup>E<sup>AR65</sup></sup>*) was used to eliminate the twinspot (Newsome et al., 2000; Stowers and Schwarz, 1999). Both F<sub>1</sub> animals and F<sub>2</sub> lines were assayed as groups of 30–50 flies using the optomotor response. After two trials, flies that failed to respond to the motion stimulus were retained. All F<sub>1</sub> animals and F<sub>2</sub> lines that displayed defects in the external morphology of the eye were discarded. FRT40A flies were used as controls. Complementation testing was performed on the homozygous lethal lines, assaying the lethal phenotype.

Single mutant R1, R6, and R7 cells were generated and labeled using GMR-FLP and the MARCM system (Lee and Luo, 2001) as described in Lee et al. (2001).

##### Histology

For labeling of all R cells, we used the R cell-specific marker mAb24B10. To label subsets of R cell types, we used the following promoters and fusions: Ro-tau-LacZ (R2-R5), PM181-Gal4 (R7, late larval stages), PANR7-Gal4 (R7, adult; Lee, et al., 2001), and Rh1-Gal4 (R1-R6, adult; Pichaud and C. Desplan, personal communication). These constructs were used to express either UAS-lacZ or UAS-synaptobrevin-GFP as noted (Estes et al., 2000). Expression of these proteins was detected using rabbit anti-lacZ (Cappel, at a 1:100 dilution) or mouse anti-GFP (Clontech, at a 1:200 dilution). To assay R cell projections at the third larval stage, we used HRP/DAB visualization as described; in all other cases, images were collected by confocal laser scanning microscopy (Bio-Rad MRC1024).

LAR protein distribution was assessed using mouse anti-LAR anti-

body (a gift from K. Zinn) at 1:10 dilution. N-cadherin protein expression was assessed using rat anti-N-cadherin (against the intracellular domain of N-cadherin, a gift from T. Uemura) at 1:20 dilution. The secondary antibodies, goat anti-rabbit or mouse or rat IgG coupled to FITC, Cy3, or Cy5 (Jackson ImmunoResearch) were used in 1:200 or 1:100 dilution. For Dil injection, see Clandinin and Zipursky (2000).

For labeling of single mutant R1 and R6 cells, the transcriptional activator Gal4 was placed under the control of a fragment of the Rh1 promoter that is expressed specifically in R1-R6 cells in the adult (Pichaud and C. Desplan, personal communication). The activity of this promoter is apparently much higher than that of the Tub-GAL80 construct used to repress GAL4 activity in the MARCM method. To limit activity of the GAL4 promoter, we performed our labeling experiments between 18°C and 20°C and assayed flies that were less than 4 days old. Under these conditions, we observe a low level of R1-R6 cell labeling independent of GMR-FLP. In control stocks lacking GMR-FLP, six labeled fibers were observed in 22 optic lobes assessed. This level of labeling is approximately 10-fold lower than that observed in congenic strains bearing the FLP construct. It is therefore possible that a small fraction of the labeled fibers seen in our experiments correspond to R1-R6 cells that are not homozygous mutant, causing us to slightly underestimate the penetrance of the defects observed in *LAR* and *N-cadherin* mutant R cells.

##### Behavioral Assay

The optomotor response and UV/Vis choice test were assayed in eye-specific mosaic flies as described in Lee et al. (2001) and Reinke and Zipursky (1988).

##### Acknowledgments

We thank members of the Zipursky lab and Utpal Banerjee for comments on the manuscript, J Treisman and B. Dickson for communication of results and reagents prior to publication, and T. Uemura, K. Zinn, E. Hafen, and C. Desplan for reagents. We thank L. Ballard for technical assistance and K. Ronan for assistance with the manuscript. This work was supported by postdoctoral fellowships from the Jane Coffin Childs Foundation (T.R.C.), the Burroughs-Wellcome Fund for Biomedical Research (T.R.C.), the Life Sciences Research Foundation (HHMI) (C.-H.L.), the Helen Hay Whitney Foundation (T.H.), and an MSTP NIH grant #GM08042 (R.L.). S.L.Z. is an Investigator of the Howard Hughes Medical Institute.

Received July 23, 2001; revised September 24, 2001.

##### References

- Ashburner, M. (1989). *Drosophila: A Laboratory Manual* (Cold Spring Harbor, NY: Cold Spring Harbor Laboratory Press).
- Brady-Kalnay, S.M., Mourtou, T., Nixon, J.P., Pietz, G.E., Kinch, M., Chen, H., Brackenbury, R., Rimm, D.L., Del Vecchio, R.L., and Tonks, N.K. (1998). Dynamic interaction of PTPmu with multiple cadherins in vivo. *J. Cell Biol.* **141**, 287–296.
- Bateman, J., Reddy, R.S., Saito, H., and Van Vactor, D. (2001). The receptor tyrosine phosphatase Dlar and integrins organize actin filaments in the *Drosophila* follicular epithelium. *Curr. Biol.* **11**, 1317–1327.
- Braitenburg, V. (1967). Patterns of projection in the visual system of the fly. I. Retina-lamina projections. *Exp. Brain Res.* **3**, 271–298.
- Burden-Gulley, S.M., and Brady-Kalnay, S.M. (1999). PTPmu regulates N-cadherin-dependent neurite outgrowth. *J. Cell Biol.* **144**, 1323–1336.
- Clandinin, T.R., and Zipursky, S.L. (2000). Afferent growth cone interactions control synaptic specificity in the *Drosophila* visual system. *Neuron* **28**, 427–436.
- Desai, C.J., Gindhart, J.G., Jr., Goldstein, L.S., and Zinn, K. (1996). Receptor tyrosine phosphatases are required for motor axon guidance in the *Drosophila* embryo. *Cell* **84**, 599–609.
- Desai, C.J., Krueger, N.X., Saito, H., and Zinn, K. (1997). Competition and cooperation among receptor tyrosine phosphatases control

- motoneuron growth cone guidance in *Drosophila*. *Development* 124, 1941–1952.
- Estes, P.S., Ho, G.L., Narayanan, R., and Ramaswami, M. (2000). Synaptic localization and restricted diffusion of a *Drosophila* neuronal synaptobrevin—green fluorescent protein chimera in vivo. *J. Neurogenet.* 13, 233–255.
- Fischbach, K.-F., and Dittrich, A.P.M. (1989). The optic lobe of *Drosophila melanogaster*. I. A golgi analysis of wild-type structure. *Cell Tissue Res.* 258, 441–475.
- Fujita, S.C., Zipursky, S.L., Benzer, S., Ferrus, A., and Shotwell, S.L. (1982). Monoclonal antibodies against the *Drosophila* nervous system. *Proc. Natl. Acad. Sci. USA* 79, 7929–7933.
- Garrity, P.A., Lee, C.H., Salecker, I., Robertson, H.C., Desai, C.J., Zinn, K., and Zipursky, S.L. (1999). Retinal axon target selection in *Drosophila* is regulated by a receptor protein tyrosine phosphatase. *Neuron* 22, 707–717.
- Gerresheim, F. (1981). Isolation and characterization of mutants with altered phototactic reaction to monochromatic light in *Drosophila melanogaster*. PhD thesis, Munich University, Munich, Federal Republic of Germany.
- Grigliatti, T. (1986). *Mutagenesis in Drosophila: A Practical Approach*, D.B. Roberts, ed. (Oxford: IRL Press), pp. 39–48.
- Heisenberg, M., and Buchner, E. (1977). The role of retinula cell types in the visual behavior of *Drosophila melanogaster*. *J. Comp. Physiol.* 117, 127–162.
- Kirshfeld, K. (1967). Die projektion der optischen umwelt auf das raster der rhabdomere im komplexauge von musca. *Exp. Brain Res.* 3, 248–270.
- Krueger, N.X., Van Vactor, D., Wan, H.I., Gelbart, W.M., Goodman, C.S., and Saito, H. (1996). The transmembrane tyrosine phosphatase DLAR controls motor axon guidance in *Drosophila*. *Cell* 84, 611–622.
- Kypta, R.M., Su, H., and Reichardt, L.F. (1996). Association between a transmembrane protein tyrosine phosphatase and the cadherin-catenin complex. *J. Cell Biol.* 139, 1519–1529.
- Laughlin, S.B., Howard, J., and Blakeslee, B. (1987). Synaptic limitations to contrast coding in the retina of the blowfly *Callifera*. *Proc. R. Soc. Lond. B* 231, 437–467.
- Lee, T., and Luo, L. (2001). Mosaic analysis with a repressible cell marker (MARCM) for *Drosophila* neural development. *Trends Neurosci.* 24, 251–254.
- Lee, C.-H., Herman, T., Clandinin, T.R., Lee, R., and Zipursky, S.L. (2001). N-cadherin regulates target specificity in the *Drosophila* visual system. *Neuron* 30, 437–450.
- Loureiro, J., and Peifer, M. (1998). Roles of Armadillo, a *Drosophila* catenin, during central nervous system development. *Curr. Biol.* 8, 622–632.
- Maurel-Zaffran, C., Suzuki, T., Gahmon, G., Tresiman, J.E., and Dickson, B.J. (2001). DLAR acts through Enabled to allow independent targeting of *Drosophila* photoreceptor axon. *Neuron* 32, this issue, 225–235.
- Meinertzhagen, I.A., and Hanson, T.E. (1993). The development of the optic lobe. In *The Development of Drosophila melanogaster*, M. Bates and A.M. Arias, eds. (Cold Spring Harbor, New York: Cold Spring Harbor University Press), pp.1363–1492.
- Newsome, T.P., Asling, B., and Dickson, B.J. (2000). Analysis of *Drosophila* photoreceptor axon guidance in eye-specific mosaics. *Development* 127, 851–860.
- O’Grady, P., Thai, T.C., and Saito, H. (1998). The laminin-nidogen complex is a ligand for a specific splice isoform of the transmembrane protein tyrosine phosphatase LAR. *J. Cell Biol.* 141, 1675–1684.
- Poeck, B., Fischer, S., Gunning, D., Zipursky, S.L., and Salecker, I. (2001). Glial cells mediate target layer selection of retinal axons in the developing visual system of *Drosophila*. *Neuron* 29, 99–113.
- Rao, Y., Pang, P., Ruan, W., Gunning, D., and Zipursky, S.L. (2000). brakeless is required for photoreceptor growth-cone targeting in *Drosophila*. *Proc. Natl. Acad. Sci. USA* 97, 5966–5971.
- Reinke, R., and Zipursky, S.L. (1988). Cell-cell interaction in the *Drosophila* retina: the bride of sevenless gene is required in photoreceptor cell R8 for R7 cell development. *Cell* 55, 321–330.
- Ren, J.M., Li, P.M., Zhang, W.R., Sweet, L.J., Cline, G., Shulman, G.I., Livingston, J.N., and Goldstein, B.J. (1998). Transgenic mice deficient in the LAR protein-tyrosine phosphatase exhibit profound defects in glucose homeostasis. *Diabetes* 47, 493–497.
- Senti, K., Keleman, K., Eisenhaber, F., and Dickson, B.J. (2000). brakeless is required for lamina targeting of R1-R6 axons in the *Drosophila* visual system. *Development* 127, 2291–2301.
- Stowers, R.S., and Schwarz, T.L. (1999). A genetic method for generating *Drosophila* eyes composed exclusively of mitotic clones of a single genotype. *Genetics* 152, 1631–1639.
- Sun, Q., Bahri, S., Schmid, A., Chia, W., and Zinn, K. (2000). Receptor tyrosine phosphatases regulate axon guidance across the midline of the *Drosophila* embryo. *Development* 127, 801–812.
- Tessier-Lavigne, M.T., and Goodman, C.S. (1996). The molecular biology of axon guidance. *Science* 274, 1123–1133.
- Tsujikawa, K., Kawakami, N., Uchino, Y., Ichijo, T., Furukawa, T., Saito, H., and Yamamoto, H. (2001). Distinct functions of the two protein tyrosine phosphatase domains of LAR (leukocyte common antigen-related) on tyrosine dephosphorylation of insulin receptor. *Mol. Endocrinol.* 15, 271–280.
- van Vactor, D. (1998). Protein tyrosine phosphatases in the developing nervous system. *Curr. Opin. Cell Biol.* 10, 174–181.
- Wills, Z., Bateman, J., Korey, C.A., Comer, A., and van Vactor, D. (1999). The tyrosine kinase Abl and its substrate enabled collaborate with the receptor phosphatase Dlar to control motor axon guidance. *Neuron* 22, 301–312.
- Zabolotny, J.M., Kim, Y.B., Peroni, O.D., Kim, J.K., Pani, M.A., Boss, O., Klamon, L.D., Kamatkar, S., Shulman, G.I., Kahn, B.B., and Neel, B.G. (2001). Overexpression of the LAR (leukocyte antigen-related) protein-tyrosine phosphatase in muscle causes insulin resistance. *Proc. Natl. Acad. Sci. USA* 98, 5187–5192.